



OPEN

Analysis of column reactor results with organic decay by native organic microbiota and varying permeability

Fernanda Costa da Silva Maciel¹, Sandro Lemos Machado^{1✉},
Antonio Fernando de Souza Queiroz² & Fernando Antonio Leite Vieira Lima¹

Field bio-remediation techniques (FBRT) can be a low cost method to avoid the removal of top layers of soil which are rich in organic matter and bio diversity. The use of native microorganisms in FBRT is preferable because non-indigenous species can transfer their genetic material to the environment with negative impacts on the local ecological equilibrium. Petroleum Produced Water (PPW) is an important pollutant source in onshore production areas. However, due to high sodium concentrations in PPW and the occurrence of organic matter in dissolved and dispersed forms, obtaining pollutant transport parameters may be a difficult task. Results of column tests performed using a natural soil permeated by PPW are presented. All the samples presented a permeability decrease over time and the total hydrocarbon petroleum (TPH) breakthrough curves presented evidence of biological decay. Soil samples underwent biological characterization after tests (Metagenomic analyses and cultural media tests). Curves were modelled in an incremental way using a non-constant decay rate to better simulate the growing process of the microorganisms and consider the occurrence of varying velocity/permeability. Biological characterization results indicate the native organisms that are potentially more able to degrade PPW, including four bacteria (*Bacillus* and *Lysinibacillus* genus) and two fungi species (*Malassezia* and *Talaromyces* genus) that have not previously been mentioned in the consulted literature. The obtained results contribute to the development of more sustainable FBRTs focusing on native microorganisms, already adapted to the local environmental conditions.

Pollutant transport parameters are very important when evaluating the impact of accidental leakages in onshore facility areas or selecting appropriated remediation technologies. Knowledge of the involved phenomena and acquisition of the necessary variables for problem modeling enable a better understanding of the transport and fate of the released pollutant components. Equation 1 can be used to describe solute transport in soils in transient fluid flow conditions¹:

$$\frac{\partial(R_d C)}{\partial t} = \nabla \cdot (\theta D_h \nabla C - v_s C) - \lambda \theta C \quad (1)$$

where C is the solute concentration ($M \cdot L^{-3}$), θ is the volumetric water content ($L^3 \cdot L^{-3}$), D_h is the hydrodynamic dispersion coefficient ($L^2 \cdot T^{-1}$), v_s is the average (macroscopic) fluid velocity ($L \cdot T^{-1}$), and t is time (T). λ is the rate constant for first-order decay (T^{-1}) and R_d is the retardation factor. D_h (refer to Eq. 2) includes the effects of both mechanical dispersion (D_m) and molecular diffusion (D^*) in soil.

$$D_h = D^* + D_m \quad (2)$$

Solute dispersion is a consequence of the heterogeneity of the soil on a microscopic scale and D_m is normally calculated as a linear function of v_s ($L \cdot T^{-1}$) (refer to Equation 3).

$$D_m = \alpha_L v_s \quad (3)$$

¹Department of Materials Science and Technology, Federal University of Bahia, Salvador 40.210-630, Brazil. ²Geo-Science Institute, Federal University of Bahia, Salvador 40.210-630, Brazil. ✉email: smachado@ufba.br

Soil sample	Particle size distribution (%)				Atterberg limits (%)				ρ_s (g · cm ⁻³)	Classification	Compaction properties normal proctor	
	Gravel	Sand	Silt	Clay	W _L	W _P	PI	A _c			USCS	w _{ot} (%)
Várzea soil ¹	1	50	14	35	48	22	26	0.74	2.73	SC	15.6	1.67
Várzea soil ²	1	55	12	32	46	25	21	0.66	2.73	SC	18.1	1.66

Table 1. Soil geotechnical characterization. Obs: A_c-soil activity; ^{1,2}: samples from first and second sampling campaigns.

Pollutant transport parameters in soil are normally evaluated using column test apparatus²⁻⁴. In some cases, however, a decrease in the soil permeability coefficient (k) has been observed despite keeping boundary conditions constant and the changes in the k values are normally attributed to physical, chemical, and biological phenomena such as filtration, bio-clogging, and clay dispersion (CD)⁵. Clay dispersion is an important theme in soil sediment, petroleum engineering and agronomy⁶⁻⁹ and occurs when soil is submitted to sodium-water flow, because sodium can deteriorate the soil structure⁷, expanding and disaggregating the clay particles and partially filling or blocking soil pores¹⁰. CD is normally pointed as the main mechanism controlling k reduction when soil is permeated by PPW, a sodium residue of petroleum production activities¹¹. Furthermore, soils permeated by PPW normally present high D_h values^{11,12} compared with those for inorganic dissolved species^{13,14}. The presence of dissolved and dispersed organic compounds in PPW tends to increase D_h values and partially justifies the very high observed α_L values¹².

The adoption of FBRT could be very attractive and low-cost and avoid the removal of most superficial soil which is usually rich in organic matter and microorganism diversity. The occurrence of highly permeable substrates, which facilitates the injection and transit of the desired microorganisms in subsurface is desirable. For superficial soil, phytoremediation technology can be used as long-term method to eliminate heavy metals¹⁵. Although the use of FBRT has drawn the attention of many researchers in recent years, the efficiency of these techniques is dependent on several environmental variables (poor capabilities of microbial communities in the field, lesser bioavailability of pollutants, growth conditions, etc.) and their use is not always suitable¹⁶. Furthermore, because the range of contaminants on which bioremediation is effective is limited, the time scales are relatively long, and the residual contaminant levels may not be acceptable^{17,18}. The use of native microorganisms is preferable to the use of non-indigenous microorganisms because they can reproduce, spread to new locations, and even transfer genetic material to microorganisms that naturally exist in the environment.

The study of microbial abundance and distribution in natural environments traditionally makes use of culture-dependent methods, which are based on metabolic and physiological characteristics. These characteristics include isolation and cultivation using solid and/or liquid media. However, with the rapid progress in molecular biology, polymerase chain reaction (PCR)-based approaches have emerged to study specific microorganisms or groups of microorganisms¹⁷.

In this paper the results of column tests performed on large samples of compacted soil are analysed to evaluate the occurrence of organic decay and their hydraulic behaviour during the percolation of PPW. The proposed experimental program consisted of performing column tests, measuring the permeability coefficient and analysing the effluent properties to plot the breakthrough curves. The chemical analyses involved the determination of parameters such as the TPH and cations concentrations, pH and electrical conductivity (EC). Furthermore, in an interdisciplinary effort, after breakthrough curve stabilization, soil samples were collected and submitted to metagenomic analyses and traditional cultural media tests to better characterize the organic processes and organisms that are involved in the degradation of PPW components.

Materials and methods

Soil. Table 1 presents the studied sediment (*Várzea soil*, VS) geotechnical characterization. VS is a fluvial sediment located on the banks of an intermittent river that crosses an onshore petroleum production area in north-east Brazil. Two sampling campaigns were performed in the field. The first campaign focused on the occurrence of clay dispersion during the tests, whereas the second campaign focused on the microorganisms that control the observed organic decay. As can be observed, the soil samples presented similar characterization results. The samples constituted a clayey sand classified as SC by USCS (Unified Soil Classification System). Complementary characterization tests, such as X-ray diffraction (XRD) (material passing on #200), X-ray fluorescence (XRF), and total volatile solids (TVS), were also performed. The main soil constituent elements (apart from oxygen) were Si = 27.8%, Al = 7.2%, Ca = 3.32%, K = 3.1%, and Cl = 3.7% whereas quartz (20.4%), kaolinite (14.2%), microcline (13.2%), and calcite (9.4%) were the main soil minerals (amorphous phase of 35.2%). An average total volatile solids value of TVS = 3.9% was obtained.

Petroleum produced water. Samples collected in the first field campaign were permeated by PPW from a nearby well. Samples from the second campaign were permeated by a synthetic PPW generated using the oil phase from the previous PPW. Table 2 presents the average PPW properties.

Column tests. Figure 1 presents the experimental apparatus. The columns are made up of a reservoir, tower and percolation column. The compacted specimens had approximate dimensions of $\phi = 20$ cm (diameter) and

Column test	TPH ($\mu\text{g/L}$)	EC ($\mu\text{S/m}$)	pH	K (mg/L)	Mg (mg/L)	Ca (mg/L)	Na (mg/L)	Salinity (mg/L)	T_s (20 °C) (mN/m)	μ (20 °C) cP
PPW ¹	2860	2540	7.0	15	45	15	277	1320	–	1.36
PPW ²	1117	2380	6.12	–	–	–	390	1350	65.1	1.35

Table 2. PPW main properties. EC = electrical conductivity; T_s = superficial tension; μ = viscosity; cP = centipoise. ^{1,2}; samples from first and second sampling campaigns.

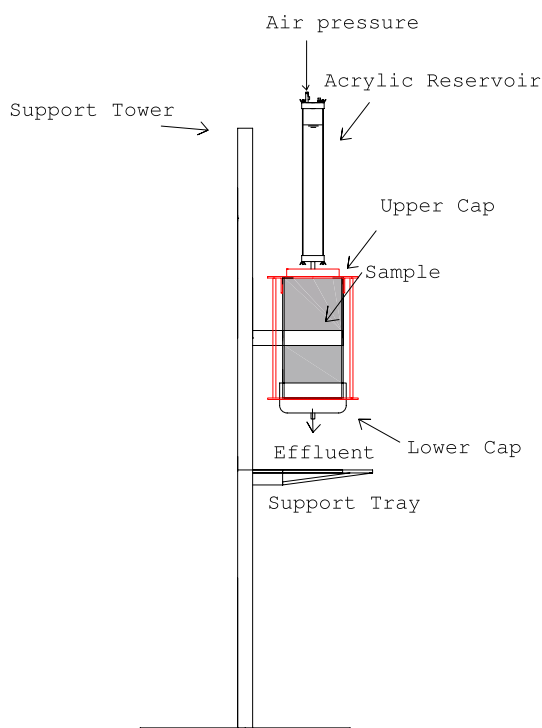


Figure 1. Sketch of the column test device.

Soil specimen	Compaction		$w - w_{ot}$	ρ_d / ρ_{dmax}	$\theta(\%)$	Sr (%)	n	Void volume (cm^3)
	w (%)	ρ_d (g/cm^3)						
CP 1 ¹	14.8	1.61	– 0.77	0.98	23.8	58.2	0.41	4736
CP 2 ¹	15.1	1.61	– 0.51	0.98	24.3	59.2	0.41	4754
CP 3 ¹	14.0	1.61	– 1.55	0.98	22.6	55.1	0.41	4749
CP 1 ²	19.1	1.66	– 1.02	1.00	31.45	80.7	0.39	5443
CP 2 ²	18.4	1.67	– 0.27	1.01	30.23	77.5	0.39	5390
CP 3 ²	19.1	1.66	– 0.96	1.00	31.36	80.4	0.39	5439

Table 3. Soil samples compaction conditions and phase relationships. ^{1,2}: samples from first and second sampling campaigns.

$L = 40$ cm (height). Before the tests, samples were saturated with water and the acrylic top reservoir was greased using PPW oil to avoid absorption of organic compounds by the tube wall. At top and bottom caps of the columns, filters composed of a mixture of coarse sand and gravel were installed. Soil samples were compacted directly inside the stainless steel body of the columns which had their inner surface previously coated with epoxy and covered with a thin layer of sand ensuring mineralogical similarity with the soil and preventing the occurrence of preferential flow paths.

Table 3 presents the characteristics of the samples after compaction. w is the gravimetric water content. All the column tests were initiated following the falling head procedure (use of atmospheric pressure on the top of the acrylic reservoir). However, owing to the observed decrease in the values of k , higher energy gradients were employed when values of permeability coefficient were lower than $1 \times 10^{-9} \text{ m} \cdot \text{s}^{-1}$. In this case, the air pressure

Soil sample	Average hydraulic head (m)	Average gradient	Average discharge of flow (m · s ⁻¹)	Time (days)
CP 1 ¹	0.70	1.75	2.8E-08	224.84
CP 2 ¹	0.72	1.80	2.4E-08	224.98
CP 3 ¹	0.78	1.94	1.8E-08	224.88
CP 1 ²	22.7	56.8	1.1E-08	194.00
CP 2 ²	42.8	106	1.2E-08	166.00
CP 3 ²	23.0	57.6	1.3E-08	230.00

Table 4. Main hydraulic characteristics of the performed column tests. ^{1,2}Samples from first and second sampling campaigns.

applied to the top of the acrylic reservoir (refer to Fig. 1) was increased. Table 4 presents additional information about the performed tests. During the tests, effluent samples were collected continuously at the base of the columns using 250 cm³ glass vials.

Effluent samples were kept at 5 °C until chemical characterization. A minimal volume of 500 cm³ (or 0.092 V_p, pore volume) was required for analytical tests (use of two consecutive samples). TPH concentrations were determined following the EPA 8015B method with the quantification of the n-alkanes (n-C12 to n-C40), isoprenoids (phytane and pristane), resolved compounds and unresolved complex mix (UCM).

Breakthrough curves ($C/C_0 \times V_p$) were fitted using Eq. (4)¹ which is the solution of Eq. (1) considering organic decay, unidirectional flow and the following boundary conditions: $C(z, 0) = 0$ p/z > 0, $C(0, t) = C_0$ p/t ≥ 0, and $C(\infty, t) = 0$ p/t ≥ 0. The equation was employed in an incremental way owing to the variations in the λ and v_s values during the tests.

$$\frac{dC}{C_0} = \frac{1}{2} \left[\frac{-2}{\sqrt{\pi}} e^{x_1} e^{-x_2^2} dx_2 + \operatorname{erfc}(x_2) e^{x_1} dx_1 \dots \right] \quad (4)$$

$$\left[-\frac{2}{\sqrt{\pi}} e^{-x_4^2} e^{x_3} dx_4 + \operatorname{erfc}(x_4) e^{x_3} dx_3 \right]$$

where

$$x_1 = \frac{(v_s - u) \cdot z}{2 \cdot D_h} \quad (5)$$

$$x_2 = \frac{R_d \cdot z - u \cdot t}{2 \cdot \sqrt{D_h \cdot R_d \cdot t}} \quad (6)$$

$$x_3 = \frac{(v_s + u) \cdot z}{2 \cdot D_h} \quad (7)$$

$$x_4 = \frac{R_d \cdot z + u \cdot t}{2 \cdot \sqrt{D_h \cdot R_d \cdot t}} \quad (8)$$

$$u = v_s \sqrt{1 + \frac{4 \cdot \lambda \cdot D_h}{v_s^2}} \quad (9)$$

In order to better simulate the growing process of the microorganisms Eq. (10)¹¹ was used to model the λ behavior during the tests.

$$\lambda = \frac{\lambda_{\max}}{1 + e^{-\beta(t-t_1)}} \quad (10)$$

where λ_{\max} corresponds to the maximum decay rate, obtained after microorganism population stabilization, β is the population growth rate, and t_1 corresponds to the time for which $\lambda = \lambda_{\max}/2$.

The following procedures were adopted to estimate the fitting variables guess values: The α_L values were estimated using Eq. (11)¹⁹.

$$\alpha_L = \frac{v_s^2}{4\pi L\omega^2} \quad (11)$$

where L is the sample length and ω is the slope of the breakthrough curve between $C/C_0 = 0.25$ and $C/C_0 = 0.5$ ($\omega = \Delta(C/C_0)/\Delta t$). The diffusion coefficient was estimated considering the PPW number of equivalent carbons, N_{ec} ²⁰. A value of $D^* = 5.1 \times 10^{-6}$ cm²/s was calculated considering $N_{ec} = 10$, value obtained from the fluid

characterization results and soil tortuosity. Due to the high α_1 values, however, the diffusion coefficient had a minor effect on the fitted results. R_d was initially set as $R_d = 1$ (minimum value considered).

A reasonable estimation for t_1 was the time necessary to reach a peak in the breakthrough curve, and the value of λ_{\max} directly influences the C/C_0 values for higher values of V_p . Appropriate β guess values were obtained according to the expression $\beta = (t_2 - t_1)^{-1}$, where t_2 corresponds to the time for which C/C_0 becomes approximately constant.

The breakthrough curves were fitted according to the minimum squares method in an interactive process (use of the Libreoffice (6.4.2) solver), applying the restriction $R_d \geq 1$. A good choice of the initial values of the fitting variables is important because the fitting process may converge to high R^2 despite using physically unrealistic combinations of the pollutant transport parameters.

Biological characterization. Biological characterization of the soil samples in the second campaign was performed. After breakthrough curve stabilization, the columns were opened and the soil samples (200 g) were collected at different depths to study the microbial abundance and diversity. Samples of *in natura* soil (reference values) were also submitted to the same procedures. Samples were quartered, and part of the collected material was frozen and stored in plastic vessels (-20°C) for genetic analysis. The remaining material was kept refrigerated in aluminum recipients for a maximum 24 h for culture and isolation tests.

The serial dilution and cultivation procedures were performed incubating the plates containing aliquots of the dilutions at 30°C for 24 h and 7 days to count the colony forming units (CFU) of bacteria and fungi, respectively²¹. Eighty-two different types of microorganisms were visually identified, isolated, and then submitted to oxidation tests (two stages)²². Tests used PPW as the carbon source, Bushnell-Haas medium (Difco), microbial suspension and redox indicator 2,6-dichlorophenolindophenol (DCPIP). Only the organisms with more than 50% efficiency in the first phase were submitted to the second phase of oxidation. Forty-one microorganisms were identified with the potential to degrade the PPW (100% of efficiency in the second phase according to the redox indicator) and submitted to DNA sequencing procedures for gender identification. Samples of PPW were submitted to the cultivation procedure. Due to the high salinity and low nutritional content of the PPW, however, it was not necessary to perform filtration or dilution procedures to obtain quantifiable CFU values of fungi and bacteria.

In the genetic identification of the microorganisms that fit the second oxidation phase requirements approximately 50 mg of cells were used in the DNA extraction method (DNeasy UltraClean microbial kit), which afford the isolation of genomic DNA from the microbial cultures. Full-spectrum NanoDrop 2000 was employed to assess the purity of the extracted DNA. The DNA amplification was performed by PCR in a Veriti thermal cycler by a reaction that employs 20 ng of purified genomic DNA. The PCR products were analysed by electrophoresis and subsequently purified with an ExoSAP-IT. The PCR products were subjected to the Sanger method for DNA sequencing.

The microbial ecology of the frozen soil samples was evaluated via amplicon metagenomics. The analysis of the soil microbiome community consisted of the direct extraction of metagenomic DNA, and its amplification was performed by the PCR technique and sequencing²³. The mixture of 10 pM of the amplifications was sequenced with MiSeq reagent 500V2 (Illumina) in the Illumina MiSeq apparatus, which generates sequences of 250 bases. DNA sequences were analysed using Quantitative Insights Into Microbial Ecology (QIME) versão 1.9.2 (Caporaso et al., 2010). The strings were grouped into Operational Taxonomic Units (OTUs) considering 97% identity with the 16S and 18S SILVA 132 database.

Results and discussion

Figure 2 presents hydraulic behaviour of the observed soil. As shown in the figure, all the samples presented a k decrease over time. Table 5 summarizes the results in terms of the initial k_i average k , and final k_f values of permeability and values of the ratio k_i/k_f . Values of k_i/k_f in the range from 3.9 to 28.3 were obtained. Figure 3 presents breakthrough curves for the main cations detected in PPW: Mg, Ca, Na, and K for sample CP2¹. As observed, after $V_p = 0.5$, the Ca concentrations present a sharp increase, while the Mg concentrations decrease and stabilize at values of $C/C_0 \approx 1$ (soil no longer releases Mg after this point). Values of $C/C_0 \approx 0$ are always obtained for Na. The obtained behaviour for the cations breakthrough curves strongly corroborates the clay dispersion hypothesis¹¹. Comparing the sampling groups, an initial sharp decrease in the values of k is observed for the samples from the second sampling campaign, which is followed by an approximately steady state phase that remains until the end of the test. The authors believe that this behaviour is probably linked to the higher sodium concentrations in the synthetic PPW.

Figure 4 illustrates the visual aspect of the collected effluent samples. Samples were enumerated according to the sampling order. Unlike the first effluent samples, samples collected at the end of the column tests presented a considerable amount of sediment at the bottom of the jars; As observed, however, clay dispersion seems to start earlier in samples from the second campaign, which is in accordance with the hydraulic behaviour presented in Fig. 2.

Figure 5 shows the obtained experimental breakthrough curves whereas Table 6 summarizes the fitting parameters using Eq. (4). As presented in the figures, organic decay can be observed in all the performed tests. Despite the fact that the curves were obtained for the same soil, the fitting parameters presented noticeable differences between sampling campaigns.

Regarding the organic decay process, higher values of t_1 and β were obtained for the samples from the second group. This delay in the development of the microbiological activities is probably linked to the lower permeability of the samples (refer to Table 5) and lower TPH concentrations in the synthetic PPW. In the case of aerobic degradation, the concentration of the substrate and transport of nutrients and oxygen in the soil are considered

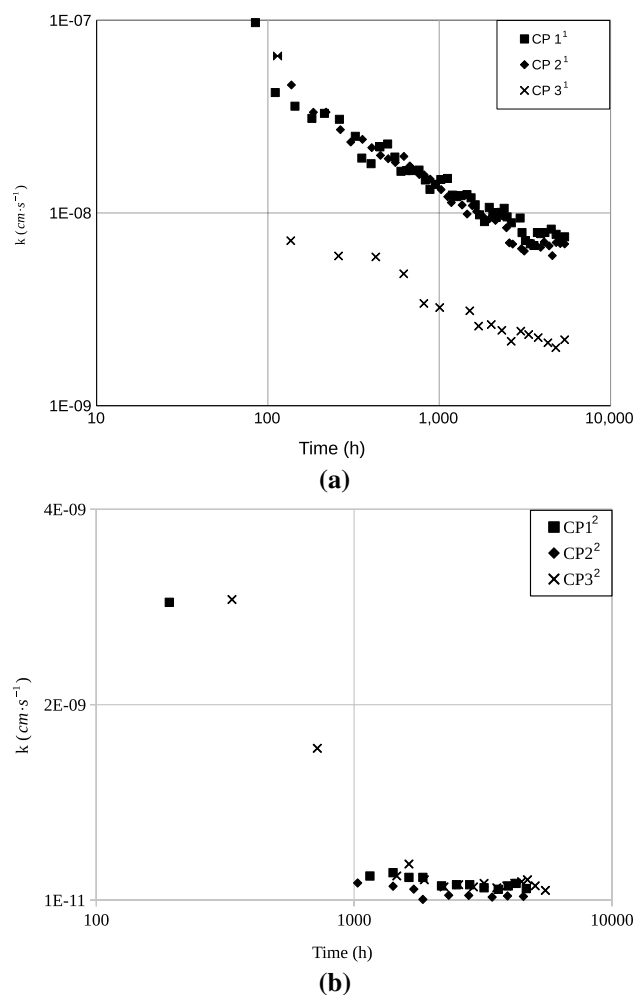


Figure 2. Permeability of soil samples. (a) First sampling campaign and (b) second sampling campaign.

Column test	k_i ($m \cdot s^{-1}$)	k_f ($m \cdot s^{-1}$)	\bar{k} ($m \cdot s^{-1}$)	k_i/k_f
CP 1 ¹	9.7E-08	5.5E-09	9.4E-09	17.8
CP 2 ¹	6.5E-08	5.4E-09	8.6E-09	12.1
CP 3 ¹	1.2E-08	1.5E-09	3.5E-09	8.4
CP 1 ²	3.1E-09	1.3E-10	4.5E-10	23.9
CP 2 ²	1.9E-10	4.8E-11	1.3E-10	3.9
CP 3 ²	3.1E-10	1.1E-10	4.6E-10	28.3

Table 5. Initial, k_i , average, \bar{k} and final, k_f soil permeability and k_i/k_f ratios.^{1,2}Samples from first and second sampling campaigns.

essential factors for the development of degradation activities. Lower permeabilities hinder the transport of these components to microbial cells and stimulate the development of anaerobic zones, which slow the degradation processes in the samples^{24–26}. The maximum decay rate (λ_{max}), however, presented a smaller intergroup variability. This seems to be more dependent on the original nature and diversity in the communities of microorganisms in the soil, which were presumably similar.

Figure 6 presents values of $D_h/D \times P_L$ obtained in the performed column tests and compares them with the curve presented by¹³, as a general trend for the ratio D_h/D^* considering data from several different authors. D_h values obtained for PPW are approximately two orders of magnitude higher than values obtained for inorganic solutes. The obtained results endorse the previously mentioned aspects concerning the behaviour of the dissolved/dispersed constituents of the PPW.

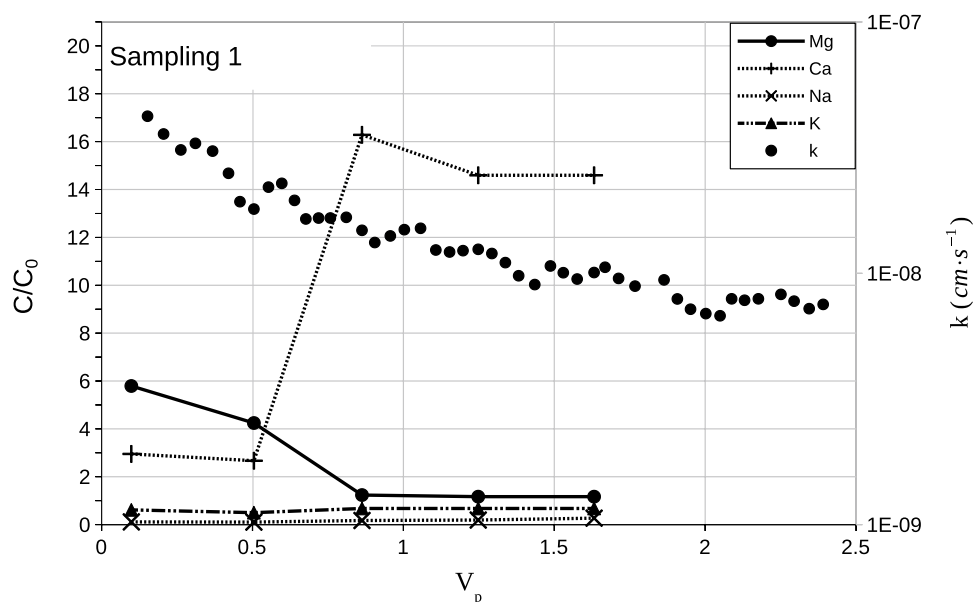


Figure 3. C/C_0 Breakthrough curves for cations and permeability.

Tables 7 and 8 present the most abundant genera obtained with the use of metagenomic techniques and compare the results with those obtained employing culture dependent methods with DNA sequencing. Lines starting with “*” indicate that the genus was identified both by metagenomic and culture dependent methods. The metagenomic analysis allowed the comparison between the soil microorganism before and after column tests. Bacteria were prevalent in relation to fungi and the most abundant genera are associated to hydrocarbon degrading activities. This was the case of the most abundant bacteria genus (*Delftia*), which is made up of aerobic bacteria which are capable of breaking down hydrocarbons of a greater molecular weight²⁷. Other examples are *Mycoplana*, *Phenylobacterium*, *Fusobacterium*, *Rhodoplanes*, *Sphingomonas*, *Methylosinus*, *Novosphingobium* and *Staphylococcus*^{28–31}. Considering the genera that could not be identified by the analysis on the QIIMI platform, the families Erythrobacteraceae, Comomonadaceae, and Xanthomonadaceae are associated with TPH decay^{32–35}. The bacteria which can potentially breakdown hydrocarbons increased in number in the column tests compared to *in natura* soil. This suggests that they play an active role in the organic decay observed.

However, mainly in the case of bacteria, some of the most abundant genera were not detected using DNA sequencing after cultivation, isolation and oxidation tests. This is because only a small percentage of bacteria and fungi can be cultivated using traditional culture techniques³⁶. Considering the culture tests performed on the fluid samples, a very low CFU number of bacteria and fungi was obtained (1,150 CFU/mL and 85 CFU/mL, respectively) compared to the tests performed in the soil samples. This indicates that the observed decay is probably due to the organisms present in the sediment.

The fungi genus *Malassezia* was the most abundant found in the metagenomic analysis, and it is one of the organisms that were able to degrade TPH in the performed oxidation tests. However, no indication in the consulted literature was obtained considering the possibility of organisms of the genus *Malassezia* degrading hydrocarbon compounds. This highlights the contribution of the present study. Considering the fungi of unidentified genus, the Eriotales, Helotiales and Agaricales orders and the family Aspergillus are reported as having hydrocarbon degrading potential. However, they did not perform well in the oxidation tests. Considering all the obtained results, four bacteria (*Bacillus* and *Lysinibacillus* genus) and two fungi species (*Malassezia* and *Talaromyces* genus) that were identified after the oxidation tests for hydrocarbon degradation have not previously been mentioned in the literature for having the ability to degrade TPH^{37–39}.

Conclusions

This paper presents results of column tests that were performed on compacted samples of a clayey sand soil permeated by PPW. The experimental results indicate the occurrence of clay dispersion in the samples with the associated decrease in soil permeability. Furthermore, all the tested samples presented the occurrence of organic decay. Breakthrough curves were modelled in an incremental way using a non constant decay rate to better simulate microorganisms growing process and consider the occurrence of varying velocity in experiments. A good adherence was obtained between experimental and modelled results. The TPH concentrations in the permeating fluid and/or soil permeability seem to influence the values of t_1 (elapsed time for which the decay rate reaches half λ_{max}) and β (rate of increase in the decay rate). The smaller variability of the maximum decay rate (λ_{max}) seems to reflect the similar original nature and diversity of the communities of microorganisms in the soil specimens⁴⁰. The obtained D_h values are substantially higher than the results presented in the technical literature concerning inorganic solutes but are compatible with previous results obtained using PPW as permeating fluid in different soils. The previously mentioned aspects are important (and most of them are



(a)



(b)

Figure 4. Photo of sampling jars containing percolated fluid. (a) First campaign and (b) second campaign.

favourable to environmental protection) when applying field remediation techniques or in the design of soil bio-barriers for PPW containment, since the VS sediment was characterized as a microbiota with potential to degrade hydrocarbons. The obtained results from the biological analysis illustrate how column tests can be performed to provide genetic material, which could be potentially applied in bio-remediation techniques that focus on native microorganisms. Furthermore, some identified species do not have a previous indication of the potential degradation of PPW compounds.

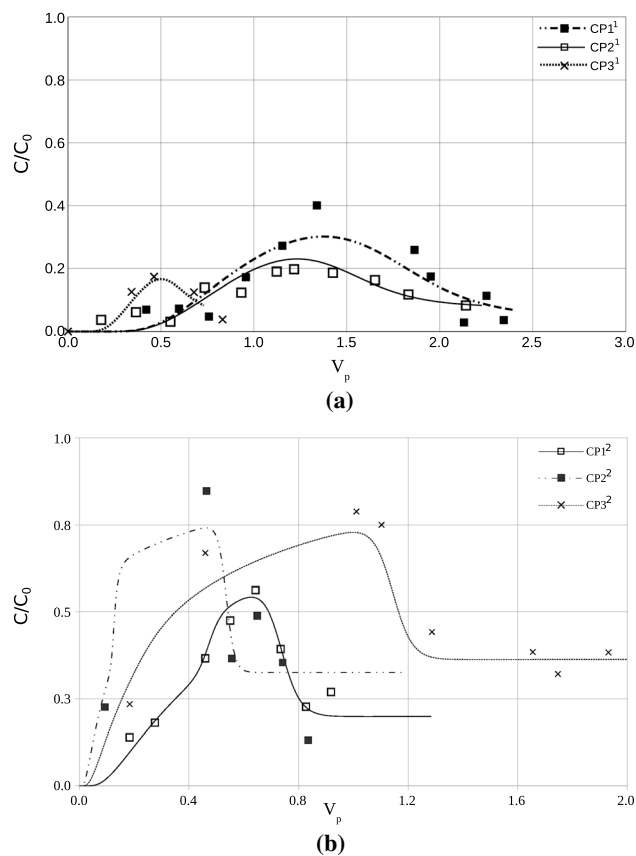


Figure 5. Experimental and fitted breakthrough curves. (a) First sampling campaign and (b) second sampling campaign.

Column test	P_L	R_d	α (m)	λ_{max} (s ⁻¹)	β (s ⁻¹)	t_1 (s)	R^2
CP 1 ¹	0.35	2.0	1.10	1.5E-06	3.0E-07	4.0E06	0.82
CP 2 ¹	0.78	1.7	0.50	9.0E-07	8.0E-07	1.0E06	0.88
CP 3 ¹	0.62	1.5	0.60	5.0E-07	3.0E-07	5.0E06	0.92
CP 1 ²	0.45	1.6	0.88	5.5E-07	2.0E-06	1.1E07	0.93
CP 2 ²	0.20	1.3	2.00	5.9E-07	5.0E-06	1.1E07	0.74
CP 3 ²	0.36	1.4	1.08	3.5E-07	2.4E-06	1.4E07	0.96
Mean		1.6	1.00	7.3E-07	1.8E-06	7.7E06	
COV		0.14	0.48	0.52	0.91	0.60	

Table 6. Obtained fitting parameters. ^{1,2}Samples from first and second sampling campaigns.

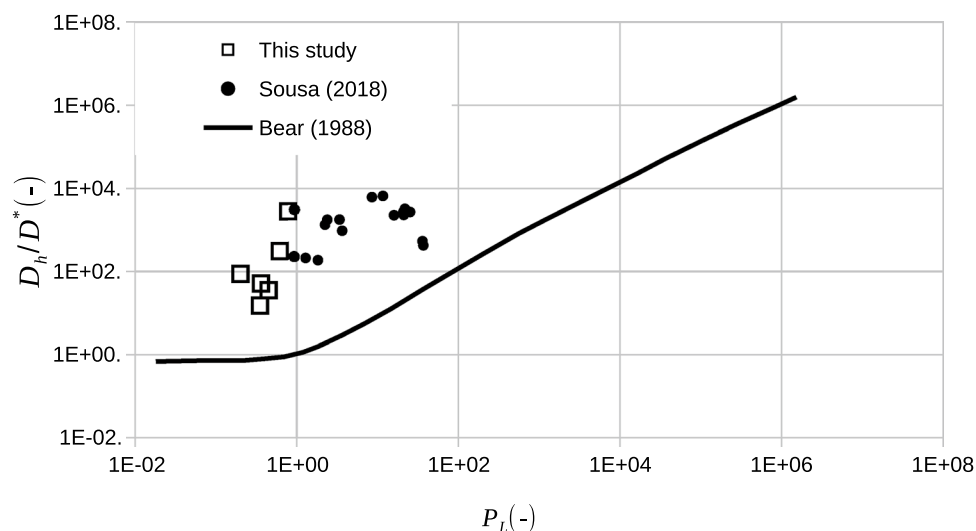


Figure 6. Hydrodynamic dispersion behaviour of column tests performed with PPW compared with values presented in the literature.

Bacteria (Order: family: genus)	CP1 ² (%)	CP2 ² (%)	CP3 ² (%)	Mean (%)	“In natura” soil (%)
Burkholderiales: Comamonadaceae: <i>Delftia</i>	66.36	70.86	71.83	69.68	65.91
Acidobacteria: Not identified: Not identified: <i>Not identified</i>	3.13	0.41	4.34	2.63	0.00
Acidobacteria: Not identified: Not identified: <i>Not identified</i>	3.52	1.93	1.63	2.36	1.11
Burkholderiales: Comamonadaceae: <i>Not identified</i>	2.16	2.23	2.26	2.22	0.00
Burkholderiales: Comamonadaceae: <i>Not identified</i>	1.83	1.71	1.92	1.82	0.00
Saprosirales: Chitinophagaceae: <i>Sediminibacterium</i>	1.02	0.02	2.58	1.21	0.06
Xanthomonadales: Xanthomonadaceae: <i>Not identified</i>	2.01	0.81	0.16	0.99	0.43
Caulobacterales: Caulobacteraceae: <i>Mycoplana</i>	2.21	0.06	0.17	0.81	0.00
Acidobacteria: Not identified: Not identified: <i>Not identified</i>	1.63	0.22	0.47	0.77	0.49
Sphingomonadales: Erythrobacteraceae: <i>Not identified</i>	0.78	0.19	1.29	0.75	0.06
Not identified: Not identified: <i>Not identified</i>	1.22	0.08	0.29	0.53	0.00
Caulobacterales: Caulobacteraceae: <i>Phenylbacterium</i>	0.26	0.55	0.23	0.35	0.13
Fusobacteriales: Fusobacteriaceae: <i>Fusobacterium</i>	0.11	0.48	0.36	0.32	0.19
Rhizobiales: Hyphomicrobiaceae: <i>Rhodoplanes</i>	0.19	0.40	0.12	0.24	0.01
Rhizobiales: Methylocystaceae: <i>Methylosinus</i>	0.06	0.03	0.40	0.16	0.05
Sphingomonadales: Sphingomonadaceae: <i>Novosphingobium</i>	0.16	0.07	0.16	0.13	0.05
Bacillales: Staphylococcaceae: <i>Staphylococcus</i>	0.09	0.21	0.02	0.11	0.09
Sphingomonadales: Sphingomonadaceae: <i>Sphingomonas</i>	0.08	0.10	0.14	0.10	0.08
*Bacillales: Bacillaceae: <i>Bacillus</i>	0.00	0.10	0.00	0.03	1.10
*Bacillales: Bacillaceae: <i>Lysinibacillus</i>	0.00	0.10	0.00	0.03	0.10
*Pseudomonadales: Pseudomonadaceae: <i>Pseudomonas</i>	0.01	0.00	0.01	0.01	0.02
*Xanthomonadales: Xanthomonadaceae: <i>Stenotrophomonas</i>	0.01	0.07	0.02	0.04	0.02

Table 7. Bacteria genera abundance.

Fungi (order: family: genus)	CP1 ² (%)	CP2 ² (%)	CP3 ² (%)	Mean (%)	"In natura" soil (%)
*Malesseiales: Incertae Sedis: <i>Malassezia</i>	12.52	18.75	31.21	20.83	17.38
Agaricomycetes: Not identified: Not identified: <i>Not identified</i>	4.33	2.34	0.42	2.36	1.34
*Eurotiales: Trichocomaceae: <i>Talaromyces</i>	1.66	1.79	3.47	2.30	7.61
Helotiales: Not identified: <i>Not identified</i>	5.71	0.00	0.00	1.90	0.00
Saccharomycetales: Incertae Sedis: <i>Candida</i>	0.00	0.00	2.31	0.77	0.00
Saccharomycetales: Not identified: <i>Not identified</i>	0.09	1.12	0.18	0.46	0.00
Pleosporales: Not identified: <i>Not identified</i>	0.74	1.95	0.00	0.90	0.00
Capnodiales: Not identified: <i>Not identified</i>	0.55	1.90	0.58	1.01	2.71
Agaricales: Not identified: <i>Not identified</i>	0.00	0.00	1.26	0.42	0.03
Onygenales: Not identified: <i>Not identified</i>	1.29	0.00	0.00	0.43	0.58
*Hypocreales: Hypocreaceae: <i>Trichoderma</i>	0.50	0.00	1.00	0.50	0.00
*Eurotiales: Trichocomaceae: <i>Aspergillus</i>	0.00	0.28	0.00	0.09	0.13

Table 8. Fungi genera abundance.

Received: 28 May 2020; Accepted: 16 February 2021

Published online: 03 March 2021

References

- Van Genuchten, M. T. & Alves, W. J. Analytical solutions of the one-dimensional convective-dispersive solute transport equation. *Tech. Rep.* [https://doi.org/10.1016/0378-3774\(84\)90020-9](https://doi.org/10.1016/0378-3774(84)90020-9) (1982).
- Patel, P., Muteen, A. & Mondal, P. Treatment of greywater using waste biomass derived activated carbons and integrated sand column. *Sci. Total Environ.* **711**, 134586. <https://doi.org/10.1016/j.scitotenv.2019.134586> (2020).
- Huang, Y., Wang, M., Gong, Y. & Zeng, E. Y. Efficient removal of mercury from simulated groundwater using thiol-modified graphene oxide/Fe-Mn composite in fixed-bed columns: Experimental performance and mathematical modeling. *Sci. Total Environ.* **714**, 136636. <https://doi.org/10.1016/j.scitotenv.2020.136636> (2020).
- Real, M., Gámiz, B., López-Cabeza, R. & Celis, R. Sorption, persistence, and leaching of the allelochemical umbelliferone in soils treated with nanoengineered sorbents. *Sci. Rep.* **9**, 1–11. <https://doi.org/10.1038/s41598-019-46031-z> (2019).
- Vandevivere, P. & Baveye, P. Relationship between transport of bacteria and their clogging efficiency in sand columns. *Appl. Environ. Microbiol.* **58**, 2523–2530 (1992).
- Moghadasi, J., Müller-Steinhagen, H., Jamialahmadi, M. & Sharif, A. Model study on the kinetics of oil field formation damage due to salt precipitation from injection. *J. Pet. Sci. Eng.* **43**, 201–217. <https://doi.org/10.1016/j.petrol.2004.02.014> (2004).
- Curtin, D., Steppuhn, H. & Selles, F. Clay dispersion in relation to sodicity, electrolyte concentration, and mechanical effects. *Soil Sci. Soc. Am. J.* **58**, 955–962. <https://doi.org/10.2136/sssaj1994.03615995005800030045x> (1994).
- Zhou, D., Wang, D., Cang, L., Hao, X. & Chu, L. Transport and re-entrainment of soil colloids in saturated packed column: effects of pH and ionic strength. *J. Soils Sedim.* **11**, 491–503. <https://doi.org/10.1007/s11368-010-0331-2> (2011).
- Waleittikil, A., Chotpanarat, S. & Ong, S. K. Impacts of salinity level and flood irrigation on Cd mobility through a Cd-contaminated soil, Thailand: experimental and modeling techniques. *J. Soils Sedim.* **19**, 2357–2373. <https://doi.org/10.1007/s11368-018-2207-9> (2019).
- Rowell, D. L., Payne, D. & Ahmad, N. The effect of the concentration and movement of solutions on the swelling, dispersion, and movement of clay in saline and alkali soils. *J. Soil Sci.* **20**, 176–188. <https://doi.org/10.1111/j.1365-2389.1969.tb01566.x> (1969).
- Lima, F. A. L. V. & Machado, S. L. Compacted soil hydraulic behaviour during the percolation of petroleum produced water. *J. Environ. Eng. Sci.* **14**, 1–12. [https://doi.org/10.1016/0378-3774\(84\)90020-9](https://doi.org/10.1016/0378-3774(84)90020-9) (2019).
- Sousa, R. G. U., de Oliveira, I. B., Machado, S. L. & de Fátima Carvalho, M. Solute dispersion of organic compounds on undisturbed soil columns. *Transp. Porous Media* **132**, 267–282. [https://doi.org/10.1016/0378-3774\(84\)90020-91](https://doi.org/10.1016/0378-3774(84)90020-91) (2020).
- Bear, J. *Dynamics of Fluids in Porous Media* (Dover Publications, INC, New York, 1988).
- Delgado, J. M. P. Q. Longitudinal and transverse dispersion in porous media. *Chem. Eng. Res. Des.* **85**, 1245–1252. [https://doi.org/10.1016/0378-3774\(84\)90020-92](https://doi.org/10.1016/0378-3774(84)90020-92) (2007).
- Zhang, Y., Wang, X. & Ji, H. Co-remediation of Pb contaminated soils by heat modified sawdust and festuca arundinacea. *Sci. Rep.* **10**, 1–13. [https://doi.org/10.1016/0378-3774\(84\)90020-93](https://doi.org/10.1016/0378-3774(84)90020-93) (2020).
- Li, W. C. & Wong, M. H. Effects of bacteria on metal bioavailability, speciation, and mobility in different metal mine soils: a column study. *J. Soils Sedim.* **10**, 313–325. [https://doi.org/10.1016/0378-3774\(84\)90020-94](https://doi.org/10.1016/0378-3774(84)90020-94) (2010).
- Varjani, S. J. & Upasani, V. N. A new look on factors affecting microbial degradation of petroleum hydrocarbon pollutants. *Int. Biodeterior. Biodegrad.* **120**, 71–83. [https://doi.org/10.1016/0378-3774\(84\)90020-95](https://doi.org/10.1016/0378-3774(84)90020-95) (2017).
- Roy, A. S. *et al.* Bioremediation potential of native hydrocarbon degrading bacterial strains in crude oil contaminated soil under microcosm study. *Int. Biodeterior. Biodegrad.* **94**, 79–89. [https://doi.org/10.1016/0378-3774\(84\)90020-96](https://doi.org/10.1016/0378-3774(84)90020-96) (2014).
- Feitosa, F. A. C., Filho, J. M., Feitosa, E. C. & Demetrio, J. G. A. *Hidrogeologia Conceitos e aplicações* 3rd edn. (CPRM, Rio de Janeiro, 2008).
- Gustafson, J. B. *Selection of Representative TPH Fractions Based on Fate and Transport Considerations* (Amherst Scientific Publishers, New York, 1997).
- Pepper, I. L. & Gerba, C. F. *Environmental Microbiology* 2nd edn. (Elsevier Academic Press, Amsterdam, 2004).
- Lima, D. F. *et al.* Isolation and selection of fungi for degrading saturated hydrocarbons, aromatic hydrocarbons and NSO compounds. *Open J. Yangtze Oil Gas* **02**, 10–26. [https://doi.org/10.1016/0378-3774\(84\)90020-97](https://doi.org/10.1016/0378-3774(84)90020-97) (2017).
- LaMontagne, M. G., Michel, F. C., Holden, P. A. & Reddy, C. A. Evaluation of extraction and purification methods for obtaining PCR-amplifiable DNA from compost for microbial community analysis. *J. Microbiol. Methods* **49**, 255–264. [https://doi.org/10.1016/0378-3774\(84\)90020-98](https://doi.org/10.1016/0378-3774(84)90020-98) (2002).
- Dhawan, S., Fan, L. T., Erickson, L. E. & Tuitemwong, P. Modeling, analysis, and simulation of bioremediation of soil aggregates. *Environ. Prog.* **10**, 251–260. [https://doi.org/10.1016/0378-3774\(84\)90020-99](https://doi.org/10.1016/0378-3774(84)90020-99) (1991).
- Yang, X., Erickson, L. E. & Fan, L. T. Dispersive-convective characteristics in the bioremediation of contaminated soil with a heterogeneous formation. *J. Hazard. Mater.* **38**, 163–185. [https://doi.org/10.1016/0304-3894\(94\)00011-50](https://doi.org/10.1016/0304-3894(94)00011-50) (1994).

26. Gogoi, B., Dutta, N., Goswami, P. & Mohan, T. K. A case study of bioremediation of petroleum-hydrocarbon contaminated soil at a crude oil spill site. *Adv. Environ. Res.* **7**, 767–782. [https://doi.org/10.1016/S1093-0191\(02\)00029-11](https://doi.org/10.1016/S1093-0191(02)00029-11) (2003).
27. Shetty, A. R. *et al.* Complete genome sequence of the phenanthrene-degrading soil bacterium *Delftia acidovorans* Cs1-4. *Stand. Genomic Sci.* **10**, 1–10. <https://doi.org/10.1186/s40793-015-0041-x2> (2015).
28. Gutierrez, T., Berry, D., Teske, A. & Aitken, M. Enrichment of fusobacteria in sea surface oil slicks from the deepwater horizon oil spill. *Microorganisms* **4**, 24. <https://doi.org/10.3390/microorganisms4030024> (2016).
29. Oldenhuis, R., Oedzes, J. Y., Van Der Waarde, J. J. & Janssen, D. B. Kinetics of chlorinated hydrocarbon degradation by *Methylosinus trichosporium* OB3b and toxicity of trichloroethylene. *Appl. Environ. Microbiol.* **57**, 7–14. <https://doi.org/10.1128/aem.57.1.7-14.19914> (1991).
30. Dong, Z. L., Wang, B. S. & Li, J. Effects of petroleum hydrocarbon contamination on soil bacterial diversity in the permafrost region of the Qinghai-Tibetan Plateau. *Soil Sedim. Contam.* **29**, 322–339. <https://doi.org/10.1080/15320383.2019.1710109> (2020).
31. Mukherjee, A., Chettri, B., Langpoklakpam, J. S., Singh, A. K. & Chattopadhyay, D. Draft genome sequence of hydrocarbon-degrading *Enterobacter cloacae* strain S1: CND1, isolated from crude oil-contaminated soil from the Noonmati oil refinery, Guwahati, Assam, India. *Genome Announc.* **4**, 3–4. <https://doi.org/10.1128/genomeA.00367-166> (2016).
32. Gutierrez, T. Aerobic hydrocarbon-degrading gammaproteobacteria: xanthomonadales. In *Taxonomy, Genomics and Ecophysiology of Hydrocarbon-Degrading Microbes* (ed. McGenity, T.) 1–15 (Springer International Publishing AG, Berlin, 2017). https://doi.org/10.1007/978-3-319-60053-6_4-17.
33. Yang, S., Wen, X., Zhao, L., Shi, Y. & Jin, H. Crude oil treatment leads to shift of bacterial communities in soils from the deep active layer and upper permafrost along the China-Russia Crude Oil Pipeline route. *PLoS One* **9**, 12–14. <https://doi.org/10.1371/journal.pone.00965528> (2014).
34. Tonon, L. A. C., Moreira, A. P. B. & Thompson, F. The prokaryotes: Alphaproteobacteria and betaproteobacteria. In *The Prokaryotes: Alphaproteobacteria and Betaproteobacteria* (eds Rosenberg, E. *et al.*) 213–235 (Springer, Berlin, 2014). <https://doi.org/10.1007/978-3-642-30197-19>.
35. Táncsics, A. *et al.* The role of beta-proteobacteria in aromatic hydrocarbon degradation: fingerprinting of 16S rRNA gene and catechol 2,3-dioxygenase gene by T-RFLP in BTEX degradative bacterial communities. In *II International Conference on Industrial, Environmental and Applied Microbiology*, 664–668. https://doi.org/10.1142/9789812837554_0138 (2009).
36. Margesin, R., Labbé, D., Schinner, F., Greer, C. W. & Whyte, L. G. Characterization of hydrocarbon-degrading microbial populations in contaminated and pristine Alpine soils. *Appl. Environ. Microbiol.* **69**, 3085–92. <https://doi.org/10.1016/j.scitotenv.2020.1366360> (2003).
37. Mohammadian, E., Arzanlou, M. & Babai-Ahari, A. Diversity of culturable fungi inhabiting petroleum-contaminated soils in Southern Iran. *Int. J. Gen. Mol. Microbiol.* **110**, 903–923. <https://doi.org/10.1016/j.scitotenv.2020.1366361> (2017).
38. Young, D. Bioremediation with white-rot fungi at Fisherville Mill: analyses of gene expression and number 6 fuel oil degradation. **1**, 89 (2012).
39. Al-Hawash, A. B., Zhang, X. & Ma, F. Removal and biodegradation of different petroleum hydrocarbons using the filamentous fungus *Aspergillus* sp. RFC-1. *Microbiologypopen* **8**, 1–14. <https://doi.org/10.1016/j.scitotenv.2020.1366362> (2019).
40. Lima, F. A. L. V. *Transporte de contaminantes oriundos da água de produção da indústria petrolífera em solos arenos-argilosos compactados*. Ph.D. thesis, Universidade Federal da Bahia, Salvador (2018).

Acknowledgements

This study was financed in part by the *Coordenação de Aperf. de Pessoal de Nível Superior-Brasil (CAPES)*-Finance Code 001.

Author contributions

F.C.S.M., S.L.M. and F.A.L.V.L. conceived the experiments. F.C.S.M. and F.A.L.V.L. performed the experiments. F.C.S.M., S.L.M. and A.F.S.Q. analysed the results. S.L.M. and A.F.S.Q. supervised and supported the work. All authors reviewed the manuscript.

Competing interests

The authors declare no competing interests.

Additional information

Correspondence and requests for materials should be addressed to S.L.M.

Reprints and permissions information is available at www.nature.com/reprints.

Publisher's note Springer Nature remains neutral with regard to jurisdictional claims in published maps and institutional affiliations.



Open Access This article is licensed under a Creative Commons Attribution 4.0 International License, which permits use, sharing, adaptation, distribution and reproduction in any medium or format, as long as you give appropriate credit to the original author(s) and the source, provide a link to the Creative Commons licence, and indicate if changes were made. The images or other third party material in this article are included in the article's Creative Commons licence, unless indicated otherwise in a credit line to the material. If material is not included in the article's Creative Commons licence and your intended use is not permitted by statutory regulation or exceeds the permitted use, you will need to obtain permission directly from the copyright holder. To view a copy of this licence, visit <http://creativecommons.org/licenses/by/4.0/>.

© The Author(s) 2021